A Tradeoff Analysis for CCD Area Imagers: Frontside Illuminated Interline Transfer vs. Backside Illuminated Frame Transfer

D. F. Barbe — Naval Research Lab. Wash., D.C. 20375

M. H. White — Westinghouse Advanced Technology Lab. Baltimore, Md. 21203

ABSTRACT: A framework for comparing CCD area arrays of different design is formulated in terms of basic systems design parameters. CCD array parameters are used to calculate the system responsivity for the backside illuminated frame transfer and the frontside illuminated interline transfer designs. Curves of system responsivity versus spatial frequency are presented.

I. INTRODUCTION

There are two basic designs for CCD low-light-level imaging chips; backside illuminated frame transfer (BIFT) and frontside illuminated interline transfer (FIIT).

In order to obtain the best possible performance from a CCD array, it is necessary to maximize the signal-to-noise ratio. The noise is basically determined by the technology used (surface channel and buried channel) and by the noise characteristics of the amplifier. On the other hand, the responsivity is largely determined by array design.

The purpose of this paper is to provide a framework for comparing CCD array of different design and to compare the BIFT and FIIT designs in detail. In order to make the comparison, we assume that the same CCD technology and amplifier technology are used for both designs.

The general framework for comparison is formulated in terms of the overall system responsivity as a function of spatial frequency. The CCD chip design parameters which affect system responsivity are then used to calculate the system responsivity for the BIFT and FIIT designs. Finally, curves of system responsivity vs. spatial frequency are plotted for comparison. The basic result is that the BIFT design gives higher responsivity at low spatial frequencies; whereas, the FIIT design gives higher responsivity at high spatial frequencies.

II. SYSTEM CONSIDERATIONS

A. CHIP RESPONSIVITY AT ZERO SPATIAL FREQUENCY

The sensor chip responsivity at zero spatial frequency, R_{CHIP}, is defined as

$$R_{CHIP} = \frac{\text{signal current out of the sensor chip}}{\text{irradiance incident on chip}} = \frac{I_s}{H}, \quad (1)$$

where the units of H are watts/m^2.

1. Narrow band excitation

For narrow band exictation between the wavelengths λ and $\lambda+d\lambda$, the signal current is

$I_s(\lambda)$ = (incident irradiance per unit wavelength)

× (incremental width of the excitation band)

× (active area of resolution element)

× (integration time)

× (energy per photon)$^{-1}$

× $\left(\frac{\text{number of electrons collected}}{\text{incident photon}}\right)$

× (charge per electron)

× (output current per electron collected)

TSMC EX. 1015 Page 1 of 8

$$= H_\lambda \, d\lambda \, \Delta x \Delta y \, t_{integ} \left(\frac{hc}{\lambda}\right)^{-1} \eta(\lambda) \, e \, \frac{g_m}{C} , \quad (2)$$

where

H_λ = irradiance per unit wavelength,

$\Delta x \Delta y$ = active area of resolution element,

t_{integ} = integration time,

$\frac{hc}{\lambda}$ = photon energy,

$\eta = \frac{\text{number of electrons collected in a resolution element}}{\text{number of photons incident on a resolution element}}$,

e = electronic charge,

g_m = transconductance of on-chip preamplifier,

C = effective capacitance at input node of the preamp.

1. Wideband Excitation

For wideband excitation, the signal current is obtained from Eq. (2) by integrating from λ_1 to λ_2:

$$I_s = \frac{g_m}{C} \Delta x \Delta y \, t_{integ} \int_{\lambda_1}^{\lambda_2} e H_\lambda \, \eta(\lambda) \frac{\lambda}{hc} \, d\lambda . \quad (3)$$

The wideband irradiance is

$$H = \int_{\lambda_1}^{\lambda_2} H_\lambda \, d\lambda . \quad (4)$$

Combining Eqs. (1), (3), and (4) gives

$$R_{CHIP} = \frac{g_m \, \Delta x \Delta y t_{integ}}{C} \frac{\int_{\lambda_1}^{\lambda_2} e H_\lambda \, \eta(\lambda) \frac{\lambda}{hc} \, d\lambda}{H} , \quad (5)$$

where $H = \int_{\lambda_1}^{\lambda_2} H_\lambda d\lambda$.

The ratio

$$R_{element} = \frac{\int_{\lambda_1}^{\lambda_2} e H_\lambda \, \eta(\lambda) \frac{\lambda}{hc} \, d\lambda}{H} , \quad (6)$$

is the responsivity of the sensor resolution element; i.e., the charge collected per joule of incident energy. Then, the chip responsivity can be written,

$$R_{CHIP} = \frac{g_m}{C} \Delta x \Delta y \, t_{integ} \, R_{element} . \quad (7)$$

B. SYSTEM RESPONSIVITY AT ZERO SPATIAL FREQUENCY

In practical applications, a lens must be used with the sensor chip, and it is the performance of the overall system which is important. The lens-sensor system is shown in Fig. 1. The symbols used in Fig. 1 are defined as follows:

W = width of the chip,
ℓ = height of the photosensitive part of the chip,
D = absolute lens aperature,
f* = lens focal length, and
θ_v = vertical field of view.

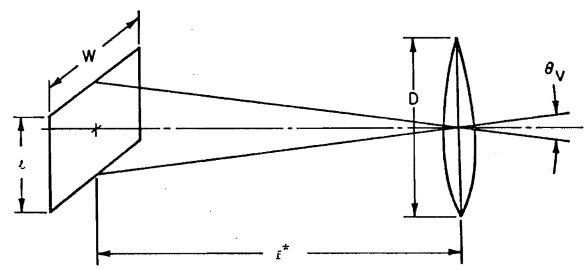

Figure 1. Schematic diagram of imaging system.

The focal ratio is defined as

$$F = f^*/D, \quad (8)$$

and the relation between chip height, focal length, and field of view is

$$\tan(\theta_v/2) = \ell/f^* . \quad (9)$$

The system responsivity at zero spatial frequency, R_{system}, is defined as

$$R_{system} = \frac{I_s}{N} , \quad (10)$$

where N is the scene radiance in W/M^2-Sr.

The sensor irradiance and scene radiance are related by Eq. (11).

$$H = \frac{N T \pi}{4F^2} , \quad (11)$$

where T is the lens transmission.

TSMC EX. 1015 Page 2 of 8

Combining Eqs. (1), (7), (10) and (11) gives the system responsivity

$$R_{system} = \frac{\pi T}{4F^2} \frac{g_m}{C} \Delta x \Delta y \, t_{integ} \, R_{element} \quad (12)$$

Equation (12) can be written more explicitly by considering the narrow-field-of-view case and the wide-field-of-view case separately.

1. Narrow-Field-of-View Case

For narrow fields of view, the limiting factor is the absolute lens aperature; thus, the focal ratio used in Eq. (12) is set by the field of view and the maximum practical lens aperature. Combining Eqs. (8), (9), and (12) gives

$$R_{system} = \frac{\pi T D^2 \tan^2(\theta v/2)}{4} \frac{g_m}{C} \times \frac{\Delta x \Delta y}{\ell^2} \, t_{integ} \, R_{element} \, . \quad (13)$$

2. Wide-Field-Of-View Case

For wide fields of view, the focal ratio is the limiting factor; thus, the focal ratio is chosen as the minimum value determined by practical lens design. The system responsivity for wide fields of view is given by Eq. (12).

C. SYSTEM RESPONSE AT NON-ZERO SPATIAL FREQUENCIES

Since most of the information content in a scene is contained in high spatial frequencies, the systems response should include a factor which takes into account the roll-off of system response with increasing spatial frequencies. This is accomplished by multiplying Eq. (12) by the MTF of the sensor chip and the MTF of the lens, i.e.,

$$R_{system}(f) = \frac{\pi T}{4F^2} \frac{g_m}{C} \Delta x \Delta y \, t_{integ} \, R_{element} \times MTF_{CHIP} \, MTF_{LENS} \, . \quad (14)$$

D. BASIS FOR COMPARING SENSOR CHIPS

The basic figure of merit of a sensor chip is the signal-to-noise ratio. In charge-coupled imagers the noise can be attributed broadly to two sources: (1) noise sources within the CCD proper, and (2) noise due to the preamplifier. The output noise current is then

$$I_n = \left[\left(\frac{q_n g_m}{C}\right)^2 + I_{npa}^2\right]^{\frac{1}{2}} , \quad (15)$$

where q_n = RMS noise charge per chip resolution element due to noise sources in front of the preamplifier, and

I_{npa} = RMS noise current due to preamplifier noise sources.

The basic figure of merit of a chip in the signal-to-noise ratio

$$\frac{I_s}{I_n} = \frac{\frac{g_m}{C} \Delta x \Delta y \, t_{integ} \, R_{element} \, MTF_{CHIP} \, H}{\left[\left(\frac{q_n g_m}{C}\right)^2 + I_{npa}^2\right]^{\frac{1}{2}}} \, . \quad (16)$$

If noise sources in front of the preamplifier dominate, then the signal-to-noise ratio is independent of g_m/C. If the preamplifier dominates, then a large g_m/C ratio is desirable. Another common way of specifying noise performance is noise-equivalent irradiance; i.e., NEI is that value of H which give $I_s/I_n = 1$.

III. CHIP CONSIDERATIONS

In this section we will discuss chip design parameters in terms of their effect on the figure of merit.

A. VERTICAL INTERLACE - INTEGRATION TIME

Figure 2 illustrates the operation of the backside illuminated frame transfer structure (BIFT) and the frontside illuminated interline transfer structure (FIIT).

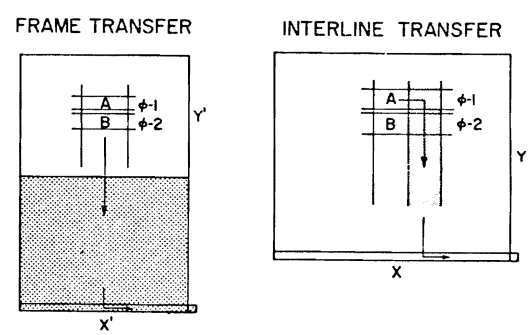

Figure 2. Diagram showing the operation of frame transfer and interline transfer chips with 2:1 interlace in the vertical direction.

TSMC EX. 1015 Page 3 of 8

In both cases two-phase structures are shown with 2:1 interlace in the vertical direction. In the frame-transfer structure, the top half of the chip is photosensitive. Field A is formed by collecting photoelectrons under the ϕ-1 electrodes for 1/60 second. This charge configuration is shifted into the shielded storage register in typically 1/600 second. Field A is then read out a line at a time while Field B is being formed by collecting photoelectrons under the ϕ-2 electrodes.

In the interline transfer structure, the shielded vertical readout registers are interdigitated with the photosensitive lines. Potential wells are formed in the photosensitive regions by applying voltages to the vertical polysilicon stripes. The horizontal polysilicon stripes are used to clock the vertical shielded registers. Because the integrating cells and shift-out cells are separate, the effective integration time for both Field A and Field B is 1/30 second. The operation is as follows: After collecting photoelectrons in Field A for 1/30 sec., the charge configuration is shifted into the shielded registers and down, a line at a time, into the horizontal output register. When Field A has been completely read out (1/60 sec), Field B is shifted into the shielded registers and out. It is important to note that the effective integration time for the interline-transfer structure is twice that of the frame-transfer structure.

Using 2:1 interlace in both structures effectively doubles the spatial sampling frequency, and the resulting Nyquist limit is $^1/p$ where p is the center-to-center distance between adjacent resolution elements on the chip (pitch).

B. MODULATION TRANSFER FUNCTION (MTF)

The MTF describes the roll-off of imager response with increasing spatial frequency. The overall MTF of the chip is composed of three factors: (1) the loss of frequency response due to the geometry of the integrating cell (MTF_{integ}); (2) the loss of frequency response due to transfer inefficiency ($MTF_{transfer}$); and (3) the loss of frequency response due to the diffusion of charge between photon absorption and photoelectron collection (MTF_{diff}). Each of these factors will be discussed separately.

1. Integration MTF

The integration MTF is given by the Fourier transform of the basic integration cell. For a rectangular cell of length Δx repeated with periodicity p, the MTF is

$$MTF_{integ} = \frac{\sin\left(\frac{f}{f_{max}} \frac{\pi\Delta x}{p}\right)}{\frac{f}{f_{max}} \frac{\pi\Delta x}{p}} , \qquad (17)$$

where $f_{max} = {}^1/p$ for 2:1 interlace. For $\Delta x = p$, the first zero in the MTF occurs at $f = f_{max} = {}^1/p$. For $\Delta x = p/2$, the first zero occurs at $f = 2\ f_{max} = {}^2/p$. Figure 3 gives the integration MTF vs. normalized spatial frequency. As shown in Figure 4, $\Delta x = \Delta y = p$ for the BIFT chip and $\Delta x = \Delta y = p/2$ for the FIIT chip.

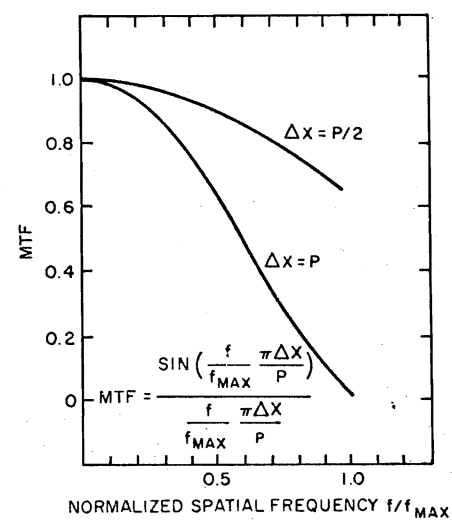

Figure 3. Integration MTF vs. normalized spatial frequency for $\Delta x = p/2$ and $\Delta x = p$.

2. Transfer MTF

During the transfer of a charge packet, Q_0, along a CCD shift register a fraction of the charge, ϵ, is lost from the packet at each transfer, and this charge $\epsilon\ Q_0$ is added to trailing charge packets. The effect of this spreading effect on MTF is given by Eq. (18).[1]

$$MTF_{transfer} = \exp\left\{-n\epsilon\left[1-\cos\left(\pi\frac{f}{f_{max}}\right)\right]\right\} . \qquad (18)$$

in a field[2] occurs when $f = {}^1/2p = {}^1/2\ f_{max}$.

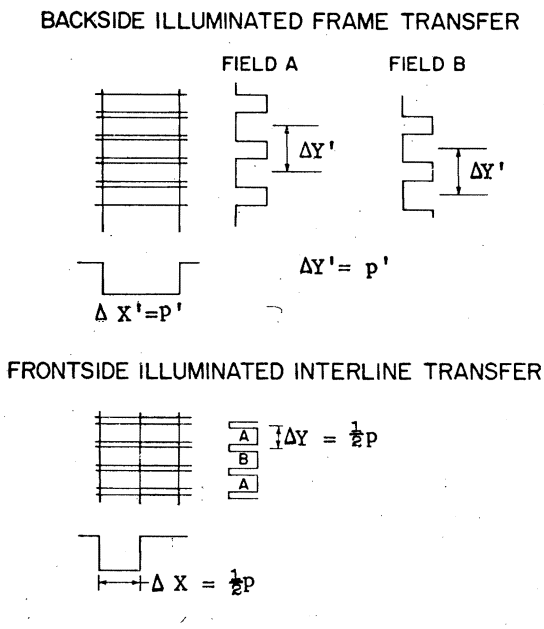

Figure 4. Diagram showing the basic integration cells for BIFT and FIIT chips.

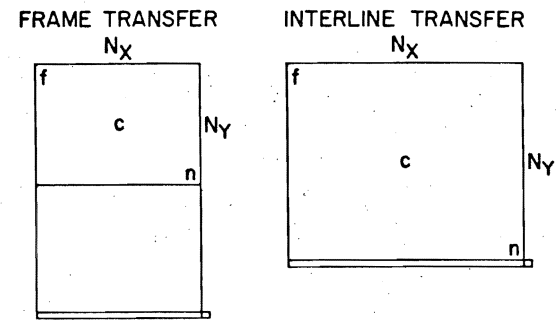

Figure 6. Frame transfer and interline transfer chips with points to indicate cell position relative to the output diode.

Figure 6 shows the frame-transfer and interline-transfer chips. N_x and N_y are the number of geometrical resolution cells in the x and y directions. Points are marked to denote cells: the farthest from the output diode (f), the center of the photosensitive array (c), and the nearest to the output diode (n).

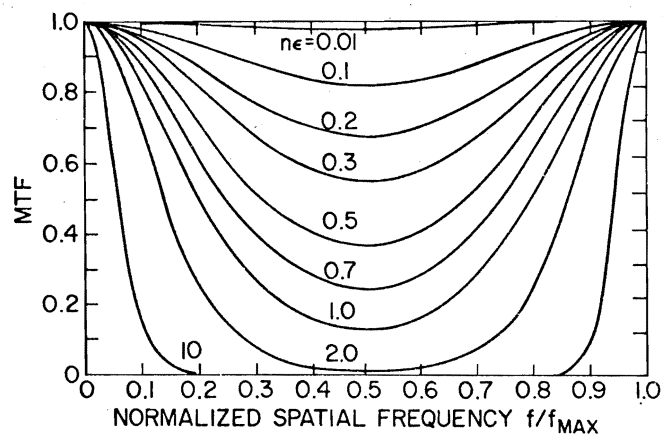

Figure 5. Transfer MTF vs. normalized spatial frequency.

Figure 5 shows the transfer MTF vs. normalized spatial frequency with the $n\epsilon$ product as the parameter. The symmetry of the curves about ${}^f/f_{max} = 0.5$ can be explained as follows. In a 2:1 interlaced array, the sampling <u>in any one field</u> occurs at spatial frequency to be sampled in f, then the frequency carried <u>in the field</u> is f for $f \leq {}^1/2p$. However, if ${}^1/2p \leq f \leq {}^1/p$, the frequency carried

Table I, gives the number of transfers required to read out the f, c, and n cells and the rates at which the charge is transferred. The number of transfers in the x-direction is the same for both frame-transfer and interline transfer arrays. Therefore, the horizontal MTF degradation due to transfer would be the same for both arrays. The number of transfers in the y-direction is greater for

TSMC EX. 1015 Page 5 of 8

Table I: Number of transfers versus position in array.

	FRAME			INTERLINE		
	f	c	n	f	c	n
AT VIDEO RATE	PN_x	$1/2PN_x$	–	PN_x	$1/2PN_x$	–
AT LINE RATE	PN_y	$1/2PN_y$	–	PN_y	$1/2PN_y$	–
AT INTERMEDIATE RATE	PN_y	PN_y	PN_y	–	–	–
TOTAL	$P(N_x + 2N_y)$	$1/2P(N_x + 3N_y)$	PN_y	$P(N_x + N_y)$	$1/2P(N_x + N_y)$	–

P = NUMBER OF PHASES

for the frame transfer chip by the amount PN_y where P is the number of phases. Therefore, the vertical MTF for the frame-transfer chip is less than that for the interline-transfer chip as given by Eq. (18).

3. Diffusion MTF

If photons are absorbed within the depletion regions, then we assume that the collection is 100% efficient. However, if photons are absorbed away from the depletion regions, then the charge configuration will spread as it diffuses toward the depletion regions with a resulting decrease in MTF.

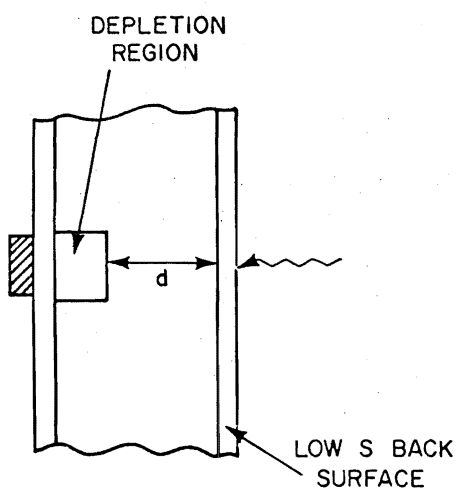

Figure 7. Diagram showing photon absorption from the backside of a thinned CCD chip.

If photons are absorbed a distance d from the depletion regions, as shown in Fig. 7, and if the diffusion length in the silicon is L_o, then the MTF due to the diffusion of charge is given by Eq. (19).[3]

$$MTF_{diff} = \frac{\text{Cosh } (d/L_o)}{\text{Cosh } (d/L)} , \qquad (19)$$

where $L^{-2} = L_o^{-2} + (2\pi f)^2$.

Figure 8 shows the diffusion MTF vs. normalized spatial frequency with d as the parameter.

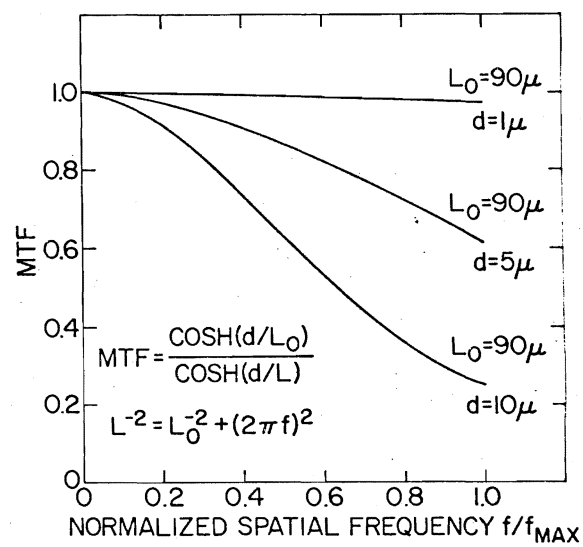

Figure 8. Diffusion MTF vs normalized spatial frequency.

C. PHOTOELEMENT RESPONSIVITY ($R_{element}$)

The photoelement responsivity is determined by the efficiency with which photons are absorbed and the resulting photoelectrons are collected. Basically four mechanisms act to reduce $R_{element}$: (1) reflection at layer interfaces before the photons reach the silicon, (2) absorption in these layers before

TSMC EX. 1015 Page 6 of 8

the photons reach the silicon, (3) recombination at the $Si\text{-}SiO_2$ interface after hole-electron generation, and (4) absorption too far away from potential wells for the photoelectrons to be collected. Mechanisms (2) and (3) cause a reduction in $R_{element}$ in the blue, mechanism (4) causes a reduction in $R_{element}$ in the infrared, and mechanism (1) causes interference fringes throughout the spectrum. Mechanism (1) is mainly responsible for $R_{element}$ being different for backside and frontside illuminated structures. Computer analysis[4] indicates that if the layer thicknesses are chosen properly, 50% of the incident photons in the 0.4-1.0 micron band are transmitted into the silicon for the frontside illuminated interline transfer structure. Therefore, $R_{element}$, averaged over the 0.4-1.0 micron band, for the FIIT structure is one half that for the BIFT structure.

IV. EXAMPLE

Suppose that an area array for a wide-field-of-view low-light-level application is to be designed with the following constraints:

(1) the distance from the object plane to the image plane, R, is specified,

(2) the vertical field of view, θ_V, is specified,

(3) the sampling distance in the object plane, G_{SD}, is to be minimized,

(4) the aspect ratio is specified, and

(5) the minimum practical focal ratio is to be used.

The problem is to determine the relative performance of the BIFT chip and the FIIT chip designed for these requirements. We assume that

(6) the largest practical chip for either design has total area A, and that

(7) the number of elements for either chip is $N_x N_y$. Table II summarizes the assumptions. The image format for the BIFT chip is X' by Y'/2 and the image format for the FIIT chip is X by Y. From (6) and (4) it follows that $Y' = 1.414Y$ and $X' = 0.707X$. From Eq. (9), it follows that $f^{*\prime} = 0.707f^*$. From the magnification relation

$$\frac{p}{G_{SD}} = \frac{f^*}{R} \quad , \tag{20}$$

it follows that $p' = 0.707p$. From Eq. (8) and constraint (5), it follows that $D = 1.414D'$.

To compare the performance of the BIFT and FIIT chips, we assume equal noise performance. Therefore, the figure of merit reduces to the system response given by Eq. (14). We also assume equal lens MTF's. Table III gives the values which are used in Eqs. (14) and (17).

Table II: Summary of the constraints for chip comparison

PARAMETER	INTERLINE TRANSFER	FRAME TRANSFER
TOTAL CHIP AREA	XY = A	X'Y' = A
ASPECT RATIO	r	r
VERTICAL FIELD OF VIEW	θ_v	θ_v
SAMPLING DISTANCE IN OBJECT PLANE	G_{SD}	G_{SD}
RANGE	R	R
NUMBER OF SENSOR CELLS	N_x, N_y	N_x, N_y
FOCAL RATIO	F	F

TSMC EX. 1015 Page 7 of 8

Table III: Values of chip parameters used in the comparison.

PARAMETER	FIIT	BIFT
ΔX	0.5 p	p'= 0.707 p
ΔY	0.5 p	p'= 0.707 p
t_{integ} (sec)	1/30	1/60
$R_{element}$	0.5	1

The results of the comparison are given in Fig. 9. At zero spatial frequency, the response of the BIFT chip is twice that of the FIIT chip. However, the response of the BIFT chip rolls off sharply and crosses the response of the FIIT chip at approximately $0.6/G_{SD}$.

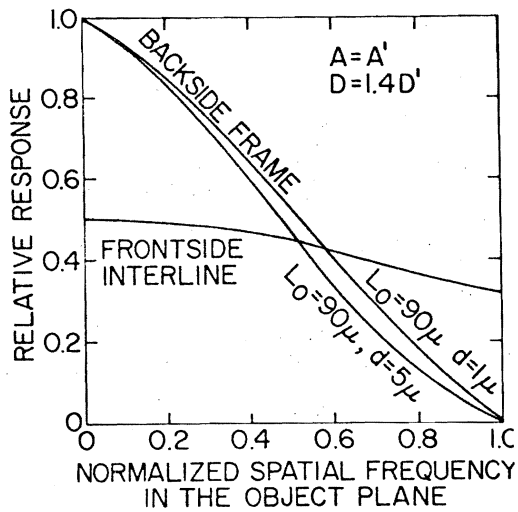

Figure 9. Relative systems response vs. normalized spatial frequency.

V. BIBLIOGRAPHY

1. G. F. Amelio, W. J. Bertram, and M. F. Tompsett, "Charge-Coupled Imaging Devices: Design Considerations," IEEE Trans. ED-18, 986 (1971).

2. C. H. Sequin, "Interlacing in Charge-Coupled Devices," IEEE Trans. ED-20, 535 (1973).

3. M. H. Crowell and E. F. Labuda, "The Silicon Diode Array Camera Diode," BSTJ 48, 1481 (1969).

4. P. Reichel, private communication.

TSMC EX. 1015 Page 8 of 8